

# Transport properties of two-dimensional electron gas in AlGaAs/GaAs selectively doped heterojunctions with embedded InAs quantum dots

H. Sakaki, G. Yusa,<sup>a)</sup> T. Someya, Y. Ohno, T. Noda,  
H. Akiyama, Y. Kadoya,<sup>b)</sup> and H. Noge

Research Center for Advanced Science and Technology, University of Tokyo 4-6-1 Komaba, Meguro-ku,  
Tokyo 153, and Quantum Transition Project, JRDC, Park Building, 4F, 4-7-6 Komaba,  
Meguro-ku, Tokyo 153, Japan

(Received 3 August 1995; accepted for publication 9 October 1995)

Transport properties of two-dimensional electron gas (2DEG) are studied in selectively doped GaAs/n-AlGaAs heterojunctions, in which nanometer-scale InAs dots are embedded in the vicinity of the GaAs channel. When the distance  $W_d$  between the InAs dot layer and the channel is reduced from 80 to 15 nm, the mobility  $\mu$  of electrons at 77 K decreases drastically from  $1.1 \times 10^5$  to  $1.1 \times 10^3$  cm<sup>2</sup>/V s, while the carrier concentration increases from  $1.1 \times 10^{11}$  to  $5.3 \times 10^{11}$  cm<sup>-2</sup>. Such a reduction of mobility is found only when the average thickness of InAs layer is above the onset level ( $\sim 1.5$  monolayer) for the dot formation. Origins of these changes in  $\mu$  and  $N_s$  are discussed in connection with dot-induced modulations of the electronic potential  $V(r)$  in the channel. © 1995 American Institute of Physics.

With the development of semiconductor technology, it has recently become possible to fabricate laterally defined nanostructures, such as quantum wires and dots. Properties of one- and zero-dimensional electrons confined in such structures have attracted a wide interest because of their importance both in physics and device applications.<sup>1,2</sup> One of the promising structures is nanometer (nm)-scale dots that can be formed by the Stranski-Krastanov mode of epitaxial growth. In this approach, a material is deposited on a lattice mismatched substrate beyond a critical thickness to form very small dot structures.<sup>3-5</sup> For example,  $\sim 20$  nm InAs dots are formed on GaAs,  $\sim 50$  nm InP dots on InGaP and  $\sim 100$  nm Ge dots on Si.<sup>3-9</sup>

In case InAs is deposited on GaAs, the first monolayer (ML) grows in the form of a fully strained two-dimensional (2D) layer. When the deposited InAs gets thicker than 1.5 ML, however, nm-scale dot structures are formed with the size fluctuation of less than 10%. It is also found that these dots are selectively formed along the edges of facet structures.<sup>10</sup> Structural and optical properties of these dots have been widely studied to clarify<sup>7,8</sup> the dot formation process, as well as quantum states of confined carriers in these dots. Very recently, capacitance spectroscopy<sup>11,12</sup> and far-infrared spectroscopy<sup>12</sup> have also been performed to disclose the details of quantum states.

Although much work has been done on the carrier confinement effect in the core part of quantum dots, relatively little is known on the influence of dot-induced potentials on the transport of electrons flowing in the neighborhood of dots.<sup>5,12-14</sup> In this work, we study, in particular, transport properties of two-dimensional electrons in GaAs/n-AlGaAs inverted heterojunctions (inverted HEMT), in which InAs

dots are embedded in the vicinity of electronic channels. We show, in particular, that both the mobility  $\mu$  and concentration  $N_s$  of electrons are strongly influenced by the presence of InAs dots, reflecting that the local potential  $V(r)$  is sensitively modulated by the dots.

Figure 1 shows schematically the structure and potential profile of selectively doped GaAs/n-AlGaAs inverted heterojunctions prepared for this work by molecular beam epitaxy (MBE) on (100) semi-insulating GaAs substrates. First, we grew at 600 °C a 200-nm-thick GaAs buffer layer and a su-

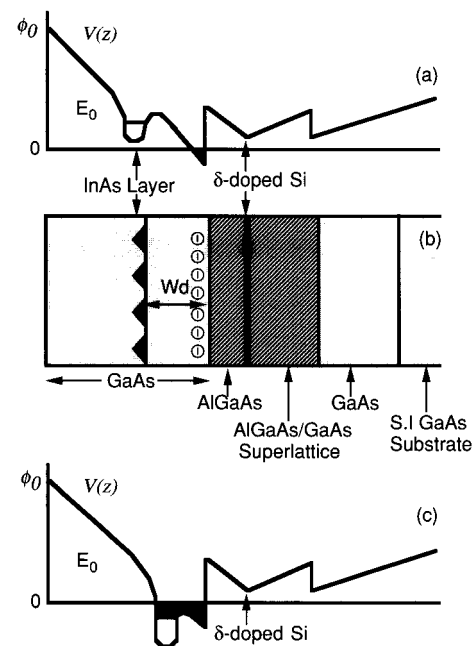


FIG. 1. Schematic illustration of the conduction band diagrams (a) and (b) and the composition profile (c) of dot-embedded single heterojunctions. Unless the dots are displaced far from the heterointerface, as shown in (b), some electrons populate dot-related quantum states, as shown in (a).

<sup>a)</sup>Electronic mail: yusa@kyokusho.rcast.u-tokyo.ac.jp

<sup>b)</sup>Present address: Department of Physical Electronics, Faculty of Engineering, Hiroshima University, Kagamiyama 1-chome, Higashihiroshima 724, Japan.

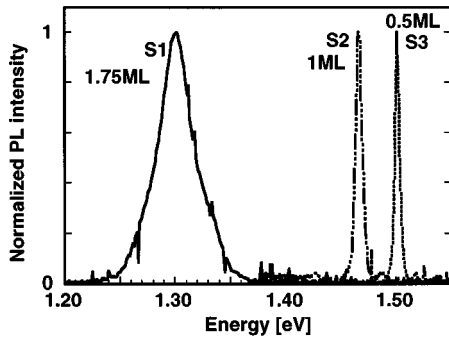


FIG. 2. Photoluminescence spectra at 17 K of three selectively doped heterojunction samples S1, S2, and S3, in which an InAs layer of 1.75, 1.0, and 0.5 ML is embedded, respectively.

perlattice containing 11 periods of a 20 nm  $\text{Al}_{0.25}\text{Ga}_{0.75}\text{As}$  and 2 nm GaAs layer. We then carried out the  $\delta$ -doping of Si with the areal concentration of  $1 \times 10^{12} \text{ cm}^{-2}$ . Because these Si atoms may outdiffuse during the growth and degrade the electron mobility in inverted heterojunctions,<sup>15,16</sup> we grew a thick (80 nm) undoped  $\text{Al}_{0.25}\text{Ga}_{0.75}\text{As}$  spacer layer at 600 °C and then deposited a GaAs channel layer. When the thickness of this GaAs layer reached a certain value  $W_d$ , which ranged from 15 to 80 nm, we reduced the substrate temperature to 450 °C within 180 s, and then deposited an InAs layer to a certain thickness  $W_{\text{InAs}}$ . We monitored the growth of InAs by *in situ* reflection high-energy electron diffraction (RHEED) and confirmed the island formation for  $W_{\text{InAs}} \geq 1.5$  ML. We performed *ex situ* atomic force microscopy (AFM) on control samples and found that the deposition of 1.75 ML InAs under our growth condition results in the dot structures of typically 8 nm in average height and 10–20 nm in average diameter at the bottom. Their concentration is about  $1 \times 10^{11} \text{ cm}^{-2}$ . To fabricate samples for our transport study, we further deposited a 2.5 nm GaAs layer (I) onto the InAs dot layer at 450 °C without growth interruption. We then raised the substrate temperature to 600 °C within 200 s and deposited the second GaAs cap layer (II) to make total thickness of the GaAs layer above the heterointerface to be 1  $\mu\text{m}$ . Note in our sample structure that InAs dots were grown after the GaAs/*n*-AlGaAs heterojunction had been formed. Hence, the intrinsic quality of our heterojunctions is expected to be as good as the reference sample with no InAs dots. The band diagrams of dot-embedded samples are schematically illustrated in Figs. 1(a) and 1(b) for two cases, in which dots are relatively close to or well-separated from the 2DEG channel, respectively. Note, that most of our samples studied here correspond to the former case where InAs dots are occupied by some electrons while additional electrons in the channel carry the current.

We studied first photoluminescence (PL) spectra to examine whether or not InAs dots were embedded as planned. We investigated three samples S1, S2, and S3, in which 1.75, 1.0, and 0.5 ML InAs layers were, respectively, embedded at  $W_d = 15$  nm from their heterojunction plane. Photoluminescence spectra measured at 17 K are shown in Fig. 2. The PL peak of sample S1 appears at 1.3 eV with the full width at

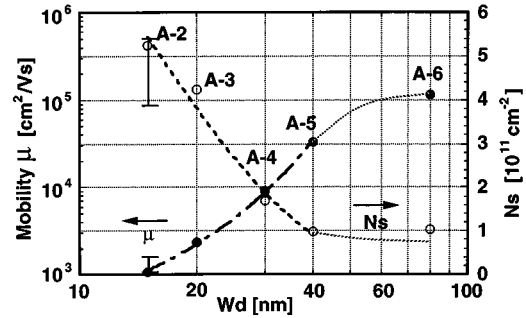


FIG. 3. Mobilities  $\mu$  and the concentrations  $N_s$  of electrons at 77 K measured as functions of  $W_d$ , the spacing between the heterojunction and the InAs dot layer. The thickness of InAs layer is 1.75 ML.

half-maximum (FWHM) of 35 meV, indicating that the InAs dots are indeed formed. No PL signal from the two-dimensional wetting layer was observed. Note also that PL spectra from samples S2 and S3 are quite sharp and appear at higher photon energies, indicating that the 0.5–1 ML thick InAs layer has grown uniformly over the wafer. In this PL study, an Ar laser with the beam diameter of 500  $\mu\text{m}$  was used for the excitation. Its power was 0.2 mW for sample S1 and 20 mW for the samples S2 and S3, respectively. Intense PL signals indicate that all the samples are of high quality.

We then studied the mobility  $\mu$  and the concentration  $N_s$  of electrons on six different samples A1–A6, in which 1.75 ML of InAs or InAs dots were embedded at different locations  $W_d$  from the interface. These samples were grown in the same MBE chamber within 2 days. We determined  $\mu$  and  $N_s$  by performing the Van der Pauw measurement at 77 K in the dark and the results are plotted in Fig. 3 as functions of  $W_d$ . Note first that  $\mu$  of sample A6 ( $W_d = 80$  nm) is quite high ( $\geq 10^5 \text{ cm}^2/\text{V s}$ ) and almost the same with  $\mu$  of reference sample without InAs dots ( $\approx 1.1 \times 10^5 \text{ cm}^2/\text{V s}$ ). Since optical-phonon-limited mobilities of electrons in selectively doped single heterojunctions are around  $2 \times 10^5 \text{ cm}^2/\text{V s}$  at 77 K, mobilities of sample A6 and reference sample are partly determined by optical-phonon scattering and partly by ionized impurity scattering. One can clearly see in Fig. 3 that mobilities drop dramatically by almost a factor of 100, as  $W_d$  decreases to 15 nm, indicating the substantial enhancement of electron scatterings. One also notices in Fig. 3 that the concentration  $N_s$  of electrons in sample A6 ( $W_d = 80$  nm) is almost the same as that ( $= 0.86 \times 10^{11}/\text{cm}^2$ ) of reference sample but  $N_s$  increases appreciably to  $5 \times 10^{11}/\text{cm}^2$  as  $W_d$  is reduced to 15 nm. Empirically, the observed dependencies of  $\mu$  and  $N_s$  on  $W_d$  can be expressed in the range of  $W_d = 15$ –40 nm as  $\mu = 141 \text{ cm}^2/\text{V s} e^{\alpha W_d}$ , with  $\alpha = 0.14/\text{nm}$  and  $N_s = 1.6 \times 10^{11} \text{ cm}^{-2} e^{\beta W_d}$ , with  $\beta = -0.071/\text{nm}$ , respectively.

To confirm that these changes of  $\mu$  and  $N_s$  originate from the dots, we also studied both  $\mu$  and  $N_s$  in a series of samples (B0–B5) where the average thickness  $W_{\text{InAs}}$  of InAs layer deposited at  $W_d = 15$  nm is varied. Figure 4 shows  $\mu$  and  $N_s$  of these samples as functions of  $W_{\text{InAs}}$ . Note that electron mobility hardly degrades as long as  $W_{\text{InAs}} \leq 1$  ML and then drastically decreases, when  $W_{\text{InAs}}$  exceeds 1.5 ML,

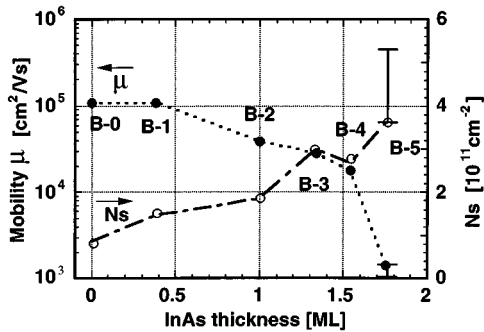


FIG. 4. Mobilities  $\mu$  and the concentration of electrons at 77 K measured in inverted heterojunction, in which an InAs layer of different thickness  $W_{\text{InAs}}$  is embedded at  $W_d = 15$  nm.

indicating that the InAs dots are the main source of mobility degradation.

These data described so far clearly indicate that the insertion of InAs dot structures give rise to new random potentials, which scatter 2D electrons very efficiently. Although the exact nature of this scattering phenomenon is not clear, we speculate that an attractive potential around each InAs dot is mainly responsible. It is because in most of our samples the wave function of electrons in the channel is strongly pulled towards the dot layer and overlaps with this potential, as shown in Fig. 1(a). Note that even when the dot-to-interface distance  $W_d$  is 40 nm, this dot-induced potential is still deep enough ( $\delta E_c \leq 300$  meV) to allow some part of the wave function to extend and overlap with the dot region. Of course, for samples with  $W_d \leq 30$  nm, this overlap is enhanced and the dot potential may even trap some of the 2D electrons. Indeed, the mobility of sample A1 with  $W_d = 0$  nm was too low to be measured, which is likely to be caused by these mechanisms.

As seen in Fig. 4, the concentration  $N_s$  of 2DEG increases from  $0.8 \times 10^{11}$  to  $5 \times 10^{11}/\text{cm}^2$ , as the thickness of the InAs layer increases, as shown in Fig. 4. Similarly,  $N_s$  is found to increase as the position of inserted dots becomes closer to the channel, as shown in Fig. 4. These increases of  $N_s$  are most likely to be caused by the InAs-induced lowering of the local conduction band edge, which enhances the electron transfer from selectively doped donors in the  $n$ -AlGaAs layer to the channel. This mechanism is similar to the enhancement effect of  $N_s$  achieved in pseudomorphic InGaAs/ $n$ -AlGaAs HEMT structures. Indeed, photoluminescence spectra of Fig. 2 indicate that the local band gap inside and around InAs dots is smaller than that of GaAs by about 200 meV, which is favorable for the enhancement of  $N_s$ .

Since each InAs dot can accommodate, at most, two electrons in its ground level, we expect that some fraction of electrons ( $\leq 1.5 \times 10^{11}/\text{cm}^2$ ) in the channel may well be trapped in the dots. In contrast, the rest of the electrons re-

main mobile, even though they are strongly scattered by InAs dots. For the precise evaluation of these trapping and scattering phenomena of electrons by InAs dots, one must assess the nature of potential  $V(r)$  around each dot by taking into account not only the change of composition but also effects of strains both inside and outside the dot. This issue will be left as the subject of a future work, because it still requires a series of experimental and theoretical studies.

Finally, we wish to emphasize that the role of unintentional impurities that have been incorporated during the growth of InAs dots should be relatively small. It is because the mobility reduction is seen only when the InAs layer exceeds 1.5 ML, which is very difficult to interpret in terms of impurities.

In summary, we have studied effects of embedded InAs dots on electron transport in selectively doped heterojunctions. We have found that the electron mobility significantly reduces at 77 K while the electron concentration increases substantially. The importance of local modulation of band edges by InAs dots is pointed out.

The authors acknowledge N. Usami for this cooperation with PL measurements. Part of this work is supported by a Grant-in-Aid for Scientific Research from the Ministry of Education, Science, Sports, and Culture, Japan.

- <sup>1</sup>H. Sakaki, Surf. Sci. **267**, 623 (1992).
- <sup>2</sup>L. Goldstein, F. Glas, J. Y. Marzin, M. N. Charasse, and G. Le Roux, Appl. Phys. Lett. **47**, 1099 (1985).
- <sup>3</sup>J. Ahopelto, A. A. Yamaguchi, K. Nishi, A. Usui, and H. Sakaki, Jpn. J. Appl. Phys. **32**, L32 (1993).
- <sup>4</sup>C. W. Snyder, B. G. Orr, D. Kessler, and L. M. Sander, Phys. Rev. Lett. **66**, 3032 (1991).
- <sup>5</sup>S. Guha, A. Madhukar, and K. C. Rajkumar, Appl. Phys. Lett. **57**, 2110 (1990).
- <sup>6</sup>R. Apetz, L. Vescan, A. Hartmann, C. Dieker, and H. Lüth, Appl. Phys. Lett. **66**, 445 (1995), and references therein.
- <sup>7</sup>D. Leonard, S. Fafard, K. Pond, Y. H. Zhang, J. L. Merz, and P. M. Petroff, J. Vac. Sci. Technol. B **12**, 2516 (1994); D. Leonard, M. Krishnamurthy, C. M. Reaves, S. P. Denbaars, and P. M. Petroff, Appl. Phys. Lett. **63**, 3203 (1993); D. Leonard, K. Pond, and P. M. Petroff, Phys. Rev. B **50**, 11687 (1994).
- <sup>8</sup>J. M. Moison, F. Houzay, F. Barthe, L. Leprince, E. Andre, and O. Vatel, Appl. Phys. Lett. **64**, 196 (1994).
- <sup>9</sup>J. Oshinowo, M. Nishioka, S. Ishida, and Y. Arakawa, Appl. Phys. Lett. **65**, 1421 (1994).
- <sup>10</sup>D. S. L. Mui, D. Leonard, L. A. Coldren, and P. M. Petroff, Appl. Phys. Lett. **66**, 1620 (1995).
- <sup>11</sup>G. Medeiros-Ribeiro, D. Leonard, and P. M. Petroff, Appl. Phys. Lett. **66**, 1767 (1995).
- <sup>12</sup>H. Drexler, D. Leonard, W. Hansen, J. P. Kotthaus, and P. M. Petroff, Phys. Rev. Lett. **73**, 2252 (1994).
- <sup>13</sup>M. Sopanen, H. Lipsanen, and J. Ahopelto, Appl. Phys. Lett. **66**, 2364 (1995).
- <sup>14</sup>I-H. Tan, R. Mirin, V. Jayaraman, S. Shi, E. Hu, and J. Bowers, Appl. Phys. Lett. **61**, 300 (1992).
- <sup>15</sup>N. M. Cho, D. J. Kim, A. Madhukar, P. G. Newman, D. D. Smith, T. Aucoin, and G. J. Iafrate, Appl. Phys. Lett. **52**, 2037 (1988).
- <sup>16</sup>L. Pfeiffer, E. F. Schubert, K. W. West, and C. W. Magee, Appl. Phys. Lett. **58**, 2258 (1991).